five monatomic gases [4], along with the results of Meyer and Sessler [5] (see Fig. 1). The experiments show that all five gases behave identically. Equation (2.13) is applied to the experimental results for $\alpha_0 = -0.12$. It is evident from Fig. 1 that agreement between theory and experiment is obtained up to $r = 0.15$, which corresponds to a Knudsen number of order unity [5].

The Predvoditelev equations can therefore be used in describing rarefied gas flows up to Knudsen numbers close to unity.

NOTATION

V, hydrodynamic velocity vector; μ, viscosity; ρ, density; γ, specific heat ratio; g_0, Laplace value of the velocity of sound; ω, cyclic frequency; c_V, specific heat at constant volume; g, phase velocity of sound; λ_{1u}, λ_{1o}, $\lambda_{1\rho}$, λ_{1T}, parameters of first-order discontinuity; λ_{2u}, λ_{2T}, parameters of second-order discontinuity; k, thermal conductivity; R, universal gas constant.

LITERATURE CITED

1. A. S. Predvoditelev, Izv. Akad. Nauk SSSR, Otd. Tekh. Nauk, No. 4 (1948).
2. V. A. Bubnov, in: Investigation of Thermohydrodynamic Light Guides [in Russian] (edited by A. V. Lykov), Izd. ITMO AN BelorusSSR (1970), p. 100.
3. A. S. Predvoditelev, in: Application of Ultrasonics to the Investigation of Matter [in Russian], No. 8, Izd. MOPI, Moscow (1959), p. 49.
4. M. Greenspan, J. Acoust. Soc. Amer., 28, 644 (1956).
5. E. Meyer and G. Sessler, Z. Phys., 149, 15 (1957).

FLOW AND HEAT TRANSFER IN A JET NEAR THE STAGNATION POINT OF A CONCAVE BODY

I. A. Belov and S. A. Isaev

UDC 536.242:532.522.2

Results are presented of calculations of flow and heat transfer near the stagnation point of a concave body in a two-dimensional subsonic jet, using a flow establishment method.

The interaction of a jet flow with blunt bodies is usually taken to mean the flow near the stagnation point, outside the region influenced by the body shape. We consider the problem of specifying such a flow near the surface of a concave body of constant curvature, located in a subsonic jet. The flow is assumed to be two-dimensional, and the fluid is assumed to be incompressible and viscous near the body surface. We restrict the analysis to a small region near the stagnation point, and represent the flow of the jet far from the surface as being approximately the flow from an ideal source.

In the body-fixed coordinate system $(\bar{\xi}, \bar{\zeta})$, (Fig. 1), where the $\bar{\xi}$ axis is tangent to the body surface, and the $\bar{\zeta}$ axis is normal to it, we select the section $\bar{\zeta} = \bar{\zeta}_\infty$, where the source flow velocity is known and equal to $\bar{V}_\infty$. We consider that the section $\bar{\zeta}_\infty$ is at a considerable distance from the obstacle, so that the effect of the obstacle on the source flow is negligibly small here. The flow is symmetric relative to the obstacle center $\bar{\xi} = \bar{\zeta} = 0$, and the external flow is irrotational; the effect of viscosity is localized in a thin boundary layer near the obstacle surface. The problem is solved in two stages. In the first stage we seek a solution in the region where the source flow and the obstacle interact $(0 \le \bar{\zeta} \le \bar{\zeta}_\infty)$, and we formulate boundary conditions for the viscous flow and heat transfer in the obstacle boundary layer. In the second stage we consider the establishment of a boundary layer on the obstacle, and determine the friction τ_W and the heat flux q_W to the surface. The problem is solved by a flow establishment method, applied to the unsteady boundary-layer equa-

Translated from Inzhenerno-Fizicheskii Zhurnal, Vol. 30, No. 2, pp. 301-309, February, 1976. Original article submitted October 4, 1974.

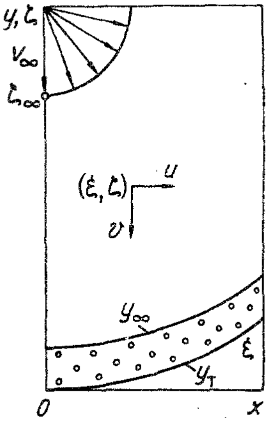

Fig. 1. Flow scheme.

tion. The obstacle surface temperature $\overline{T}_W$ and the external flow temperature $\overline{T}_\infty$ are considered constant.

1. We consider flow from an ideal source near the stagnation point $\overline{\xi} = \overline{\zeta} = 0$, which coincides with the center of the obstacle (Fig. 1). The equations determining this flow have the form

$$\frac{\partial u}{\partial \xi} + \frac{\partial}{\partial \zeta}[v(1 - K\zeta)] = 0, \tag{1}$$

$$\frac{\partial v}{\partial \xi} - \frac{\partial}{\partial \zeta}[u(1 - K\zeta)] = 0, \tag{2}$$

where $u, v = [(\overline{u}, \overline{v})/\overline{V}_\infty]$; $\xi, \zeta = [(\overline{\xi}, \overline{\zeta})/\overline{\xi}_\infty]$; u and v are the velocity components along the ξ and ζ axes, respectively; and K is the curvature of the obstacle $(0 < K < 1)$.

Near the stagnation point we seek a solution for u and v in the form

$$u = \xi f'(\zeta), \quad v = -f(\zeta)/(1 - K\zeta).$$

The function $f(\zeta)$ was determined from Eq. (2),

$$f''/f' = K/(1 - K\zeta) \tag{3}$$

with the following boundary conditions:

$$\zeta = 0, \quad f = 0; \quad \zeta = 1, \quad f = 1 - K.$$

Then for u and v we obtain

$$u = \xi K(K - 1)/\ln(1 - K)(1 - K\zeta), \tag{4}$$

$$v = (K - 1)\ln(1 - K\zeta)/\ln(1 - K)/(1 - K\zeta). \tag{5}$$

2. For the analysis of the flow and heat transfer in the boundary layer we use a rectangular coordinate system $(\overline{x}, \overline{y})$, with origin at the obstacle center $\overline{x} = \overline{y} = 0$. We adopt the notation $\eta = (\overline{y} - \overline{y}_T)/(\overline{y}_\infty - \overline{y}_T)$, where $\overline{y}_\infty$ is the thickness of the viscous layer $\overline{y}_T$ on the obstacle surface. With this notation the system of equations describing the flow and heat transfer in the boundary layer has the form

$$\frac{\partial U}{\partial x} - \frac{\partial U}{\partial \eta} \cdot \frac{y'_T}{y_\infty - y_T} + \frac{\partial V}{\partial \eta} \cdot \frac{1}{y_\infty - y_T} = 0; \tag{6}$$

$$\frac{\partial U}{\partial t} + U\frac{\partial U}{\partial x} + V\frac{\partial U}{\partial \eta} \cdot \frac{1}{y_\infty - y_T} - U\frac{\partial U}{\partial \eta} \cdot \frac{y'_T}{y_\infty - y_T} = -\frac{\partial p}{\partial x} + \frac{\partial^2 U}{\partial \eta^2} \cdot \frac{1}{(y_\infty - y_T)^2}; \tag{7}$$

$$\frac{\partial T}{\partial t} + U\frac{\partial T}{\partial x} + V\frac{\partial T}{\partial \eta} \cdot \frac{1}{y_\infty - y_T} = \mathrm{Ec}\,\frac{\partial^2 U}{\partial \eta^2} \cdot \frac{1}{(y_\infty - y_T)^2} + \frac{1}{\mathrm{Pr}} \cdot \frac{\partial^2 T}{\partial \eta^2} \cdot \frac{1}{(y_\infty - y_T)^2} + U\frac{\partial T}{\partial \eta} \cdot \frac{y'_T}{y_\infty - y_T}, \tag{8}$$

where

$$U = \frac{\overline{U}}{\overline{V}_\infty}; \quad V = \frac{\overline{V}}{\overline{V}_\infty}; \quad T = \frac{\overline{T}}{\overline{T}_\infty}; \quad p = \frac{\overline{p}}{\rho \overline{V}_\infty^2}; \quad x = \frac{\overline{x}}{\overline{\xi}_\infty};$$

$$\eta = \frac{\bar{y} - \bar{y}_T}{\bar{y}_\infty - \bar{y}_T}; \quad y = \frac{\bar{y}\sqrt{\mathrm{Re}}}{\bar{\zeta}_\infty}; \quad t = \frac{\bar{t}\bar{V}_\infty}{\bar{\zeta}_\infty}.$$

We solve Eqs. (6)-(8) with the following boundary conditions:

$$t > 0, \ \eta = 0, \quad U = V = 0, \quad T = T_w = \mathrm{const},$$
$$\eta = 1, \quad U = U(x, 1), \quad T = T_\infty = 1, \tag{9}$$

and at t = 0 we use Eqs. (4) and (5) for the velocity components in the coordinate system (x, η)

$$U = v \sin\vartheta + u \cos\vartheta, \quad V = (v \cos\vartheta - u \sin\vartheta)\sqrt{\mathrm{Re}},$$

where

$$u = -\frac{\vartheta \sin\vartheta}{Kx}\Phi(K), \quad v = -\frac{\ln(Kx/\sin\vartheta)}{Kx/\sin\vartheta}\Phi(K),$$
$$\vartheta = \mathrm{arctg}(Kx/(1 - Ky)), \quad \Phi(K) = (1 - K)/\ln(1 - K),$$
$$y = [y_T + (y_\infty - y_T)\eta]/\sqrt{\mathrm{Re}},$$

and the fluid temperature is assumed constant and equal to $T = T_\infty = 1$.

In order to find an additional boundary condition for the V component of velocity on the axis of symmetry (x = 0), we represent the solution for the U velocity component in the immediate vicinity of the symmetry axis in the form [1]

$$U = xU1(t, x, \eta),$$
$$\frac{\partial U}{\partial x} = U1(t, x, \eta) + x\frac{\partial U1}{\partial x}, \quad \left.\frac{\partial U}{\partial x}\right|_{x=0} = U1(t, 0, \eta).$$

Similarly, we write an expression for the velocity at the outer edge of the boundary layer, for $\eta = 1$,

$$U_0 = U(x, 1) = xU1_0(t, x),$$
$$\frac{\partial U_0}{\partial x} = x\frac{\partial U1_0}{\partial x} + U1_0, \quad \left.\frac{\partial U_0}{\partial x}\right|_{x=0} = U1_0.$$

Taking into account these relations, from the Bernoulli equation we find

$$-\frac{\partial p}{\partial x} = xU1_0^2 + O(x^2).$$

Then Eqs. (6) and (7) for x = 0 can be written in the form

$$U1 + \frac{1}{y_\infty - y_T} \cdot \frac{\partial V}{\partial \eta} = 0, \tag{10}$$

$$\frac{\partial U1}{\partial t} + V\frac{\partial U1}{\partial \eta} \cdot \frac{1}{y_\infty - y_T} = \frac{1}{(y_\infty - y_T)^2} \cdot \frac{\partial^2 U1}{\partial \eta^2} - U1^2 + U1_0^2. \tag{11}$$

The boundary conditions for solving Eqs. (10) and (11) for U1 and V are

$$\eta = 0, \quad U1 = 0, \quad V = 0,$$
$$\eta = 1, \quad U1 \to U1_0. \tag{12}$$

Since the fluid in the boundary layer is incompressible, this system of equations is solved separately for the dynamic and thermal problems.

3. In order to construct a finite-difference analog for the above system of equations we divide the region of integration into a number of cells $\Delta x = Q$, $\Delta\eta = H$. Then $x = (i - 1)Q$, $\eta = (j - 1)H$. We introduce a time step Δt, such that $t = m\Delta t$. We use forward differences for the time derivatives and central differences for the derivatives with respect to x and η. Equations (6) and (7) in finite-difference form can be written as

$$[U_{i,j}^{m+1} - U_{i,j}^m]/\Delta t + U_{i,j}^m[U_{i+1,j}^m - U_{i-1,j}^m]/(2Q) + V_{i,j}^m[V_{i,j+1}^m -$$
$$- V_{i,j-1}^m]/(2H)/(y_\infty - y_T) = -\partial p/\partial x + [U_{i,j+1}^m + U_{i,j-1}^m - 2U_{i,j}^m]/H^2/(y_\infty - y_T)^2 + U_{i,j}^m y_T'[U_{i,j+1}^m - U_{i,j-1}^m]/(2H)/(y_\infty - y_T), \tag{13}$$

$$[U_{i,j-1}^{m+1} - U_{i-1,j-1}^{m+1} + U_{i,j}^{m+1} - U_{i-1,j}^{m+1}]/(2Q) + [V_{i-1,j}^{m+1} - V_{i-1,j-1}^{m+1} +$$
$$+ V_{i,j}^{m+1} - V_{i,j-1}^{m+1}]/(2H)/(y_\infty - y_T) = y_T'[U_{i-1,j}^{m+1} - U_{i-1,j-1}^{m+1} + U_{i,j}^{m+1} - U_{i,j-1}^{m+1}]/(2H)/(y_\infty - y_T). \tag{14}$$

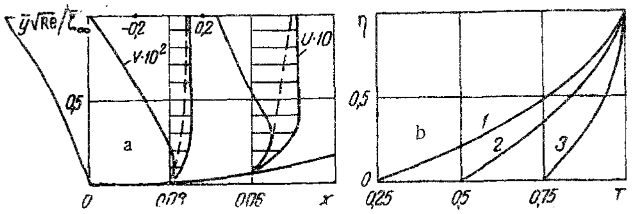

Fig. 2. Velocity profiles (a) in the obstacle boundary layer with K = 0.4; Re = 10^4 (solid curve); the Hiemenz for K = 0 [3] (broken line) and temperature profile (b) in the obstacle boundary layer for K = 0.4; Re = 10^4; Ec = 0; Pr = 1.0; 1 − T_W = 0.25; 2−0.5; 3−0.75

$$[U1_j^{m+1} - U1_j^m]/\Delta t = [U1_{j+1}^m + U1_{j-1}^m - 2U1_j^m]/H^2/(y_\infty - y_T)^2 - [U1_j^m]^2 - V_{1,j}^m[U1_{j+1}^m - U1_{j-1}^m]/(2H)/(y_\infty - y_T), \tag{15}$$

$$V_{1,j+1}^{m+1} = V_{1,j-1}^{m+1} - 2HU1_j^{m+1}(y_\infty - y_T). \tag{16}$$

In choosing relations between Δt, Δx, and Δη, we used the following stability conditions for the boundary-layer equations in finite-difference form [2]:

$$\Delta t \leqslant 1/(U_{i,j}^m/\Delta x + 2/(\Delta\eta)^2),\quad \Delta\eta \leqslant 2/V_{i,j}^m. \tag{17}$$

Equations (13)-(16) with boundary conditions (9) and (11) were solved using the following scheme.

1. At time t = 0 we consider U and V to be equal to the corresponding values obtained from solution of the ideal problem.

2. At time Δt from Eq. (15) we find U1, from the known values at time t = 0. Then, using an iteration method, taking into account the boundary conditions on the obstacle surface, from Eq. (16) we find the V component of velocity on the axis of symmetry,

$$V_{1,j+1}^{(k+1)} = V_{1,j+1}^{(k)} + \omega\,[V_{1,j-1}^{(k)} - U1_j 2H(y_\infty - y_T) - V_{1,j+1}^{(k)}],$$

where the index k denotes the iteration number, and ω is a relaxation coefficient, assumed equal to 1.85. After satisfying the condition $|V_{1,j}^{(k+1)} - V_{1,j}^{(k)}| < \epsilon$, at the control points, where ε is the allowable error in the solution, we recalculate the velocity gradient on the axis of symmetry,

$$U1_j = -[V_{1,j+1} - V_{1,j-1}]/(2H)/(y_\infty - y_T),$$

which is used in the calculations at the next time step.

3. Solution of Eqs. (13) and (14) at time Δt for x > 0 is carried out analogously.

4. We repeat operations 2 and 3 at successive times to obtain the established solution.

During the solution we determine the velocity field in the boundary layer and the friction on the obstacle surface,

$$\tau_w = \frac{\bar{\tau}_w}{\bar{\rho}V_\infty^2} = \frac{1}{\sqrt{\mathrm{Re}}}\left[\frac{(1-Ky)^2}{K^2x^2+(1-Ky)^2}\cdot\frac{\partial U}{\partial y}\bigg|_{y=y_T} + \frac{1}{\mathrm{Re}}\cdot\frac{K^2x^2}{K^2x^2+(1-Ky)^2}\cdot\frac{\partial V}{\partial x}\bigg|_{y=y_T}\right].$$

For a small region near the stagnation point the friction is assumed to be approximated by the expression

$$\tau_w = \frac{1}{\sqrt{\mathrm{Re}}}\cdot\frac{\partial U}{\partial y}\bigg|_{y=y_T} = \frac{1}{\sqrt{\mathrm{Re}}}\cdot\frac{1}{y_\infty - y_T}\cdot\frac{\partial U}{\partial \eta}\bigg|_{\eta=0}. \tag{18}$$

The time of flow establishment is determined by obtaining a value for the friction on the obstacle surface which repeats with a given accuracy.

In solving the thermal problem we use the earlier results of calculating the velocity in the boundary layer. Equation (8), in finite-difference form, has the form

$$[T_{i,j}^{m+1} - T_{i,j}^m]/\Delta t + U_{i,j}[T_{i+1,j}^m - T_{i-1,j}^m]/(2Q) + V_{i,j}[T_{i,j+1}^m - T_{i,j-1}^m]/(2H)/(y_\infty - y_T) = U_{i,j}[T_{i,j+1}^m - T_{i,j-1}^m]/(2H)/(y_\infty - y_T)\,y_T' + \mathrm{Ec}\,[U_{i,j+1} + U_{i,j-1} - 2U_{i,j}]/H^2/(y_\infty - y_T)^2 + [T_{i,j+1}^m + T_{i,j-1}^m - 2T_{i,j}^m]/H^2/\mathrm{Pr}/(y_\infty - y_T)^2. \tag{19}$$

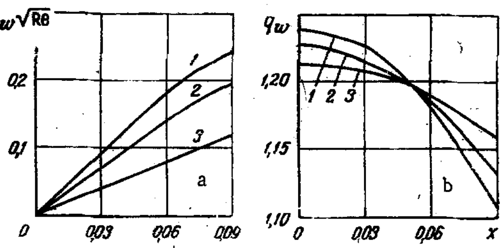

Fig. 3. Distribution of friction factor (a) and heat flux (b) near the stagnation point of the obstacle for $Re = 10^4$; $Pr = 1.0$; $Ec = 0$; $T_W = 0.25$; $1 - K = 0.2$; $2 - 0.4$; $3 - 0.6$.

There are no particular difficulties in solving Eq. (19) for $T_{i,j}^{m+1}$, with constant temperature conditions at the obstacle surface and at the outer edge of the boundary layer. The initial values for temperature and velocity in the boundary layer at time $t = 0$ were assumed to be as follows: $T = 1$, and U and V have their values at the time of flow establishment in the boundary layer. During the solution the temperature field in the boundary layer was determined. From the well-known law for temperature distribution in the boundary layer, we further calculated the heat flux from the fluid to the wall:

$$q_w = \frac{\bar{q}_w \bar{\zeta}_\infty}{\bar{\lambda}\bar{T}_\infty} = \frac{1 - Ky}{\sqrt{K^2x^2 + (1 - Ky)^2}} \sqrt{\mathrm{Re}} \frac{\partial T}{\partial y}\bigg|_{y=y_T} - \frac{Kx}{\sqrt{K^2x^2 + (1 - Ky)^2}} \cdot \frac{\partial T}{\partial x}\bigg|_{y=y_T}.$$

For a small region near the stagnation point the latter expressions take the form

$$q_w = \sqrt{\mathrm{Re}} \frac{1}{y_\infty - y_T} \cdot \frac{\partial T}{\partial \eta}\bigg|_{\eta=0}. \tag{20}$$

The time for establishment is the same as in calculating friction, and was determined by obtaining a value of heat flux to the obstacle which repeated with time with a given accuracy.

5. The dynamic and thermal problems were solved on the BÉSM-4 computer. In both cases the same 21×21 computational mesh was used. The initial data chosen were: $H = 0.05$; $Q = 0.025$; $\Delta t = 10^{-6}$ (the first 25 steps) and $\Delta t = 10^{-4}$ (subsequent steps); $y_\infty = 1.0$; $\epsilon = 10^{-5}$; $T_W = 0.25, 0.5$, and 0.75; $Re = 10^4$; $Ec = 0$; $Pr = 1.0$. The body curvature varied in the range $0 < K < 1$. Some of the computer results, obtained at the time assumed for the solution to establish, are shown in Figs. 2-4.

Figure 2a shows the profiles of the U and V velocity components at the time of flow establishment in the boundary layer on an obstacle with curvature $K = 0.4$, at time step 131 for $Re = 10^4$. We note that, unlike flow near the stagnation point of a two-dimensional obstacle normal to a uniform external stream [3], for flow over an obstacle of concave shape there is a layer near the surface where the V component changes sign; the U velocity component profile is close to the theoretical Hiemenz profile for flow of a uniform stream over a perpendicular obstacle [3], but differs in magnitude from the latter. The broken curve in Fig. 2a corresponds to the Hiemenz solution $U = U(\varphi)$, where $\varphi = \sqrt{\bar{\beta}/\nu}\bar{y}$, $\bar{\beta}$ is the velocity gradient at the stagnation point. Since the flow velocity at the outer edge of the boundary layer near the stagnation point for two-dimensional and concave obstacles is given by the linear relation $\bar{U} = \bar{\beta}\bar{\xi}$, in terms of the coordinate over the obstacle surface ξ, it follows from solution of the problem of interaction of a perfect stream with an obstacle that the velocity gradient at the stagnation point of the obstacle is $\bar{\beta} = K(K-1)\bar{V}_\infty/\bar{\zeta}_\infty/\ln(1-K)$, and for $K \to 0, \beta \to \bar{V}_\infty/\bar{\zeta}_\infty$. Typical profiles of the temperature in the boundary layer near the stagnation point are shown in Fig. 2b for $K = 0.4$; $Re = 10^1$; $Ec = 0$; $T_W = 0.25$ (curve 1); $T_W = 0.5$ (curve 2); $T_W = 0.75$ (curve 3).

Figure 3a shows the distribution of the established wall friction in the form $\tau_W\sqrt{Re} = f(x)$ for $Re = 10^4$ and $K = 0.2$ (curve 1), for $K = 0.4$ (curve 2), and for $K = 0.6$ (curve 3). Figure 3b gives the heat flux distribution over the obstacle surface under the same conditions in flow with $Ec = 0$; $T_W = 0.25$.

It is interesting to compare the results obtained with the friction and heat flux values near the stagnation point, determined for a uniform stream normal to a two-dimensional flat plate obstacle. In this case, we can write the following expression [3] for the friction:

$$\tau_{w\,f.p} = \frac{\bar{\tau}_{w\,pl}}{\bar{\rho}\bar{V}_\infty^2} = C\frac{\bar{U}\sqrt{\bar{\beta}\bar{\nu}}}{\bar{V}_\infty^2} = \frac{\xi C}{\sqrt{\mathrm{Re}}},$$

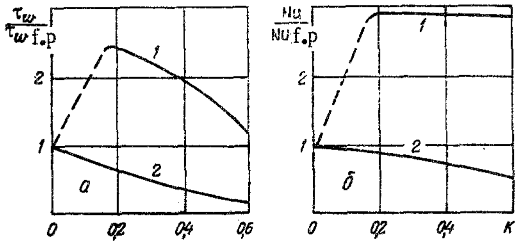

Fig. 4. Ratios of the friction (a) and the heat flux (b) at the stagnation point of a concave obstacle to the corresponding flat plate values [3]: 1) present calculation; 2) calculation using relations for a flat plate normal to a uniform stream, corrected for the velocity gradient at the stagnation point of the concave obstacle.

where

$$\bar{U} = \bar{V}_\infty \xi, \quad \beta = \bar{V}_\infty / \bar{\xi}_\infty, \quad C = 1.23259.$$

The data presented in Fig. 3a show that $\tau_w\sqrt{Re}$ is a linear function of ξ near the stagnation point for a concave obstacle: $\tau_w\sqrt{Re} = C_1\xi$, where $C_1 = f(K)$, and, therefore, the ratio $\tau_w/\tau_{w\,f.p} = C_1/C$. Taking into account the values obtained for C_1, the ratio $\tau_w/\tau_{w\,f.p}$ for $Re = 10^4$ is shown in Fig. 4a (curve 1). If we use the formula for the friction near the stagnation point of a plate washed by a uniform normal stream in calculating the friction on a concave obstacle, i.e., if we compute only the variation in the velocity gradient at the stagnation point of the obstacle because of the curvature, then we obtain

$$\tau_w/\tau_{wf.p} = [K(K-1)/\ln(1-K)]^{1.5},$$

as follows from the expression for the velocity gradient at the stagnation point of a concave obstacle. The results of the calculation using this formula are shown in Fig. 4a (curve 2). Similarly, we can compare the heat flux at the stagnation point of a concave obstacle and on a plate washed by a uniform normal stream. In the latter case we have [3]

$$Nu_{f.p} = \frac{\bar{\alpha}_{f.p}\bar{\xi}_\infty}{\bar{\lambda}} = C_2\sqrt{Re},$$

where $C_2 = 0.57\,Pr^{0.4}$; $\bar{\alpha}_{f.p}$ is the coefficient of heat transfer for the plate. For a concave obstacle, from Eq. (20) we obtain

$$Nu_{f.p} = \frac{\bar{\alpha}\bar{\xi}_\infty}{\bar{\lambda}} = \frac{\bar{T}_\infty}{\bar{T}_\infty - \bar{T}_w} q_w,$$

where $\bar{\alpha}$ is the heat-transfer coefficient for a concave obstacle. Taking the latter expressions into account, the ratio $Nu/Nu_{f.p}$ has the form

$$\frac{Nu}{Nu_{f.p}} = \frac{T_\infty}{C_2(T_\infty - T_w)} \cdot \frac{q_w}{\sqrt{Re}}.$$

Using numerical values for q_w (Fig. 3b), obtained with $Re = 10^4$; $Ec = 0$; $Pr = 1.0$; $T_w = 0.25$, the ratio $Nu/Nu_{f.p}$ is shown in Fig. 4b. If the heat flux near the stagnation point of a concave obstacle is calculated using the formula for q_w for a plate washed by a uniform normal stream, i.e., if in a case with friction we calculate only the variation in the velocity gradient at the stagnation point of a concave obstacle, in comparison with the gradient at the plate stagnation point we obtain

$$\frac{Nu}{Nu_{f.p}} = C_2\sqrt{\frac{K(K-1)}{\ln(1-K)}}\sqrt{Re}.$$

The results of the calculation using the latter formula are shown in Fig. 4b (curve 2).

The investigation conducted here allows us to conclude that the friction and heat flux near the stagnation point of a concave body depend appreciably on the obstacle curvature. For the range of curvature investigated, $0.2 \le K \le 0.6$, the friction and heat flux near the stagnation point of a concave obstacle are greater by a factor of 2.5 than the corresponding values for a flat plate washed by a uniform normal stream. A calculation of friction and heat flux at the stagnation point of a concave obstacle, using relations for a two-dimensional flat plate, accounting for variation in the velocity gradient at the stagnation point of the obstacle, gives underestimated values (by a factor from 3 to 8), compared with the present results.

NOTATION

ξ, ζ, axes of the body-fixed coordinate system; ζ_∞, distance from the obstacle at which the effect of the obstacle and the outer flow is negligibly small; x, y, rectangular coordinate system axes; y_∞, thickness of viscous layer on the obstacle; y_T, coordinate of the obstacle surface; η, transformed coordinate; t, time; ϑ, slope angle of the velocity vector V_∞ to the axis of symmetry; u, v, velocity components along the axes ξ, ζ in the region of interaction of an ideal flow with the obstacle; U, V, velocity components along the x and y axes in the obstacle boundary layer; V_∞, velocity at section ζ_∞; U1, gradient of U in direction x; β, velocity gradient at the obstacle stagnation point; ρ, density; T, temperature; T_W, wall temperature; T_∞, temperature of outer flow; p, pressure; μ, dynamic viscosity; λ, thermal conductivity; c_p, specific heat; α, heat-transfer coefficient; K, curvature of obstacle; τ_W, friction on the obstacle surface; q_W, heat flux to the obstacle surface; Q, H, sizes of computational mesh cell in the direction of the x and η axes, respectively; Δt, time step; i, j, m, cell numbers in the directions x, η, and t; k, iteration number; w, relaxation coefficient; $Re = \bar{\rho}\bar{V}_\infty\bar{\zeta}_\infty/\bar{\mu}$, Reynolds number; $Pr = \bar{c}_p\bar{\mu}/\bar{\lambda}$, Prandtl number; $Ec = \bar{V}_\infty^2/(\bar{c}_p\bar{T}_\infty)$, Eckert number; $Nu = \alpha\zeta_\infty\lambda$, Nusselt numbers. Indices: 0, parameters at the outer edge of the boundary layer; f.p, parameters on a two-dimensional flat plate, positioned normal to a uniform external stream; –, dimensional value.

LITERATURE CITED

1. V. M. Paskonov, in: Some Applications of the Mesh Method, No. 1 Boundary-Layer Flows [in Russian], Izd. MGU (1971).
2. C. L. S. Farn and V. S. Arpaci, AIAA J., 4, 730 (1966).
3. I. P. Ginzburg, Theory of Hydraulic Resistance and Heat Transfer [in Russian] Izd. LGU (1970).

MECHANISM OF BOILING ON SUBMERGED SURFACES WITH CAPILLARY-POROUS COATING

O. N. Man'kovskii, O. B. Ioffe, L. G. Fridgart, and A. R. Tolchinskii

UDC 536.423.1

An approximate model is proposed for the process of boiling in a porous layer. The model shows satisfactory qualitative and quantitative agreement with experimental data over a wide range of heat fluxes.

Heat-transfer surfaces with capillary-porous coatings have been arousing much interest among researchers, since boiling seems to occur on them somewhat more intensely than on uncoated surfaces. In particular, it has been noticed that boiling on porous surfaces may occur for very small temperature differences, hence permitting the transfer of large heat fluxes in thermodynamically favorable conditions.

The study of this phenomenon is known to present certain difficulties, since its mechanism is determined by heat-transfer processes that occur inside the structure of the capillary-porous layer, where they are inaccessible to visual observation and direct measurement. Probably as a result, the literature has so far lacked any general methods allowing the calculation and analysis of this process on the basis of specified properties of the medium, parameters of the porous layer, the characteristics of the coating material, and the temperature difference. Experimental results and empirical correlations were presented in [1-3],

Translated from Inzhenerno-Fizicheskii Zhurnal, Vol. 30, No. 2, pp. 310-316, February, 1976. Original article submitted December 2, 1974.